

Lagrangian Structures in Very High-Frequency Radar Data and Optimal Pollution Timing

Francois Lekien*, Chad Coulliette*[†] and Jerry Marsden*

*Control and Dynamical Systems, California Institute of Technology, Pasadena, CA 91125

[†]Environmental and Engineering Science, California Institute of Technology, Pasadena, CA 91125

Abstract. Very High-frequency (VHF) radar technology produces detailed surface velocity maps near the surface of coastal waters. The use of measured velocity data in environmental prediction, however, has remained unexplored. In this paper, we uncover a striking flow structure in coastal radar observations along the coast of Florida. This structure governs the spread of organic contaminants or passive drifters released in the area. We compute the Lyapunov exponents of the VHF radar data to determine optimal release windows in which contaminants are advected efficiently away from the coast and we show that a VHF radar-based pollution release scheme using the hidden flow structure reduces the effect of industrial pollution in the coastal environment.

INTRODUCTION

The release of pollution in coastal areas [1, 2, 3] can lead to dramatic consequences for local ecosystems if the pollution recirculates close to the coast rather than being transported out to the open ocean and safely absorbed. We demonstrate that sensitivity to initial conditions in coastal flows can create different patterns of behavior for released contaminants. Depending on their release position and release time, identical parcels of contaminants can have completely different effects on the environment. Using a combination of accurate current measurement [4] and recent developments in nonlinear dynamical systems theory [5, 6], we uncover previously unknown flow structures¹ that govern the mesoscale transport of pollutants. Knowledge of these Lagrangian structures should lead to predictions [7] on a number of phenomena, ranging from the motion of plankton populations to the evolution of oil spills. In this paper we demonstrate how Lagrangian structures can be exploited to reduce the damaging effects of coastal pollution.

We describe fluid particle motion as a dynamical system obeying:

$$\dot{\mathbf{x}} = \mathbf{v}(\mathbf{x}, t) . \quad (1)$$

In contrast to earlier approaches to optimal pollution release in simple flow models [8, 9, 10, 11, 12], we rely on real-time data obtained directly from coastal radar antennas. To determine the velocity, the left-hand side of Equation (1), we examine very

¹ By flow structure we mean Lagrangian structures, i.e. sets of distinguished fluid particles moving along with the flow.

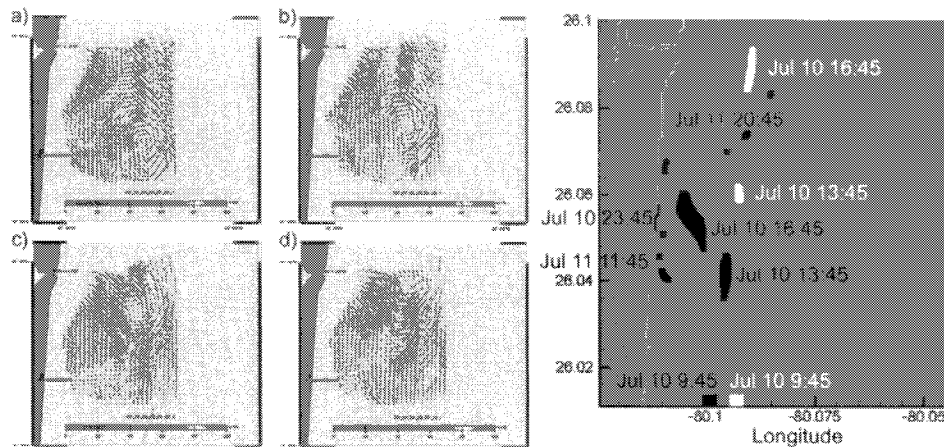


FIGURE 1. On the left, surface current images of the velocity pattern obtained by HF radar along the coast of Florida, near Fort Lauderdale from SFOMC 4-D Current Experiment on June 26, 1999: a) 01:20 GMT; b) 02:20 GMT; c) 04:00 GMT; d) 05:20 GMT. On the right, two parcels of contaminant released at exactly the same time, but at slightly different initial locations on July 10, 1999 at 09:45 GMT. The white parcel leaves the domain quickly and dissolve in the open ocean. The black parcel re-circulates near the coast for more than 36 hours. Animation: <http://www.transport.caltech.edu/florida.html>

high-frequency (VHF) radar measurement of near-surface currents along the coast of Florida [4]. Except for measurement errors, the VHF data shown on Fig. 1 is an exact footprint of the actual velocity as described by Equation (1).

VHF RADAR DATA ALONG THE COAST OF FLORIDA

The OSCAR VHF model [13, 14] was deployed for the Southern Florida Ocean Measurement Center (SFOMC) 4-Dimensional Current Experiment from June 25-August 25, 1999. Radio waves are backscattered from the moving ocean surface by surface waves of one-half of the incident radar wavelength. This Bragg scattering effect [15] results in two discrete peaks in the Doppler spectrum. In the absence of surface current, spectral peaks are symmetric and their frequencies are offset from the origin by an amount proportional to the surface wave phase speed and the radar wavelength. If there is an underlying surface current, Bragg peaks in the Doppler spectrum are displaced by the radial component of current along the radar's look direction. Using two radar stations sequentially transmitting radio waves resolves the two-dimensional velocity vector for placing the data into a geophysical context.

The two transmit/receive stations operated at 50 MHz and sent electromagnetic signals scattered from surface gravity waves with 3-m wavelengths. Coastal ocean currents were mapped over a $7 \text{ km} \times 8.5 \text{ km}$ domain at 20 minute intervals with a resolution of 250 m. The radars were located in John Lloyd State Park, Dania Beach (Master) and an oceanfront site in Hollywood Beach (Slave) which equated to a distance of 7 km.

NUMERICAL EXPERIMENTS

The temporal complexity of the currents becomes evident from tracking different evolutions of a fluid parcel² released at the same time, but at a slightly different location. We show the results of two such numerical experiments on Fig 1. The complete animation and others can be downloaded from <http://www.transport.caltech.edu/florida.html>. We have performed this analysis using two parcels of particles launched at 09:45 GMT on July 10, 1999. Using available VHF velocity data, we advected the fluid particles using a 4th order Runge-Kutta-Fehlberg algorithm (RK45) combined with a 3rd order tricubic interpolation in both space and time³.

Note that the black contaminant parcel remains near the coast, whereas the white parcel exits the domain quickly to the North and advects into the open ocean. The latter scenario is highly desirable, because it minimizes the impact of the contaminant on coastal waters, by causing it to be safely dispersed in the open ocean. This observation inspires us to understand and predict different evolution patterns of a fluid parcel, depending on its initial location and time of release. Such patterns are known to be delineated by repelling material lines or finite-time stable manifolds [16, 17, 18, 19, 20, 21]. Here we shall use a recently developed nonlinear technique, Direct Lyapunov Exponent [6] (DLE) analysis, which identifies repelling or attracting material lines in velocity data as local maximizing curves of material stretching.

LAGRANGIAN COHERENT STRUCTURES

The DLE algorithm starts with the computation of the flow map, the map that takes an initial fluid particle position \mathbf{x}_0 at time t_0 to its later position $\mathbf{x}(t, \mathbf{x}_0)$ at time t . To perform this analysis, we launched a grid of 200×200 particles at time t_0 . Using a 3rd order interpolation of the VHF radar data, we advected the particles of the grid for $t - t_0 = 25$ hours, using a 4th order Runge-Kutta-Fehlberg algorithm. We used these particle trajectories to approximate the flow map. We modeled the coastline as a free-slip boundary, and disregarded particles that crossed the open boundaries of the domain on the northern, eastern and southern edges. All of these numerical algorithms have been compiled into a software package, MANGEN, that is available from the authors upon request.

We then compute the largest singular value $\sigma_t(\mathbf{x}_0, t_0)$ of the spatial gradient of the flow map [21]. More specifically, we compute the largest eigenvalue of the Cauchy-Green strain tensor

$$\Sigma_t(\mathbf{x}_0, t_0) = \left[\frac{\partial \mathbf{x}(t, \mathbf{x}_0)}{\partial \mathbf{x}_0} \right]^T \left[\frac{\partial \mathbf{x}(t, \mathbf{x}_0)}{\partial \mathbf{x}_0} \right], \quad (2)$$

with the superscript T referring to the transpose of a matrix.

² A fluid parcel is a simplified model for a blob of contaminant.

³ The resulting local interpolator provides a C^1 velocity field in extended phase space.

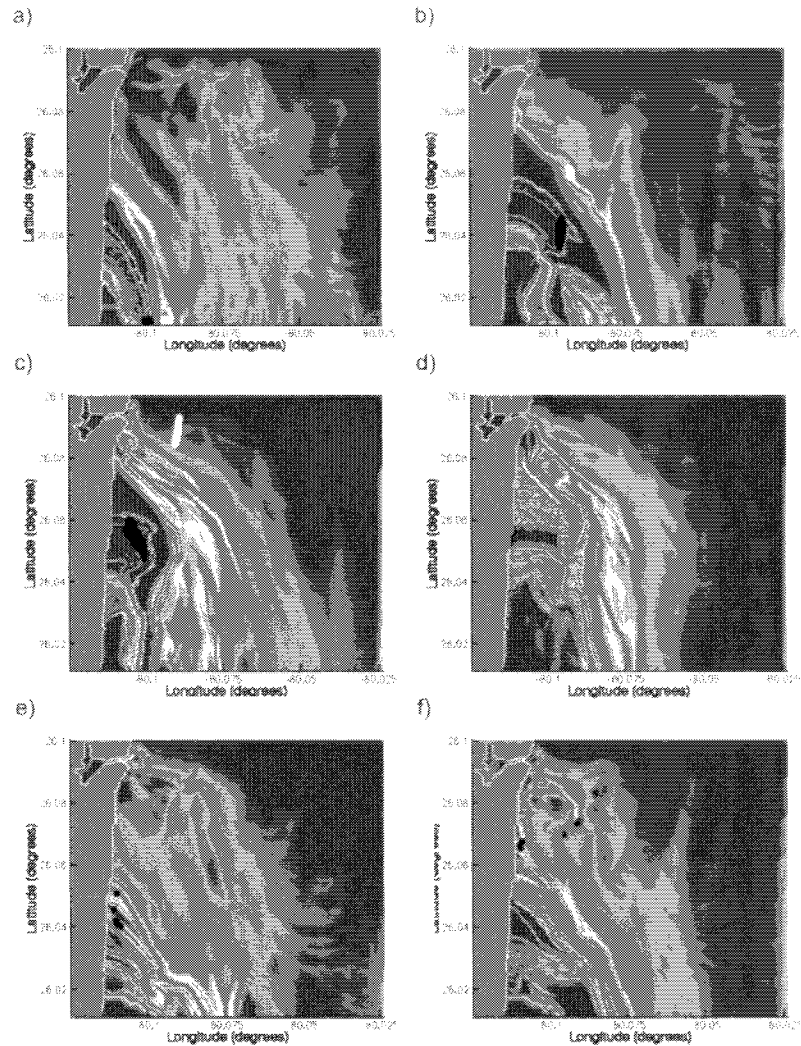


FIGURE 2. Level Sets of Direct Lyapunov Exponents along the coast of Florida on (a) July 10, 1999 09:45 GMT, (b) July 10 13:45 GMT, (c) July 10 16:45 GMT, (d) July 10 23:45 GMT, (e) July 11 11:45 GMT and (f) July 11 20:45. The simulation clearly shows a stable manifold (i.e. repelling material line) attached to the coast near Fort Lauderdale. Superimposed on each figure panel are the respective positions of the two parcels from Fig. 1. Every particle north of the manifold flows through the northern open boundary. It is non-optimal to release contaminants below the branch of the manifold because it will remain between the coast and the manifold for a long time. *Animation:* <http://www.transport.caltech.edu/florida.html>

Repelling material lines are local maximizing curves or ridges of the scalar field $\sigma_t(\mathbf{x}_0, t_0)$ [6, 22]. The same procedure performed backward in time (i.e., for $t < t_0$) would render attracting material lines at t_0 as ridges of $\sigma_t(\mathbf{x}_0, t_0)$.

Composed of fluid particles, these curves remain hidden to naked-eye observations of unsteady current plots, yet they fully govern global mixing patterns in the fluid. Such Lagrangian structures in measured ocean data have previously been inaccessible due to lack of an efficient extraction method.

ANALYSIS OF THE DATA

Selected frames of the contour level sets of the Lyapunov exponents are shown in Fig. 2. During the two months of the experiment, the plot reveals a strong stable Lagrangian structure attached to the coast near Fort Lauderdale, propagating to the southeast. This structure acts as a Lagrangian barrier between the coastal recirculating zone (southwest of the material line) and the Florida Current (northeast of the same material line). The material line is a barrier in the sense that particles cannot cross it. Superimposed on Fig. 2 are the two parcels used in Fig. 1. A quick analysis reveals that any particle northeast of the barrier (white parcel) is flushed out of the domain in only a few hours. In contrast, parcels starting southwest of the barrier (black parcel) typically re-circulate several times near the Florida coast before they finally rejoin the current. The animation corresponding to the panels of Fig. 2 can be downloaded at <http://transport.caltech.edu/florida.html>. It is important to realize that without the use of DLE or a similar method, the Lagrangian structure would still be there, but could not be seen or made use of in this way. We prefer to think of the currents as not influencing particle paths directly, but rather that the currents influence the Lagrangian structure, such as causing transport barriers and alleyways, and the Lagrangian structure directly influences the particle paths.

MINIMIZATION OF THE EFFECT OF POLLUTION

We remark that the location of the base of the structure (on the coast) can be used as a criteria to minimize the effect of coastal pollution. We will refer to the intersection of the coastline and the Lagrangian structure as the barrier point. Factories and sewing centers along the coast should not release anything if the barrier point is located North of them. To illustrate how an efficient pollution release algorithm can be set up, we imagined a source of pollution with a fixed position along the coast. Using the DLE plots of Fig. 2, we identify zones of (light gray) favorable release⁴ and (dark gray) dangerous release⁵.

To minimize the effect of coastal pollution, we propose using a holding tank that stores contaminants during dangerous release zones. The tank stores pollution during

⁴ when the manifold is below the position of the factory

⁵ when the manifold is above the factory

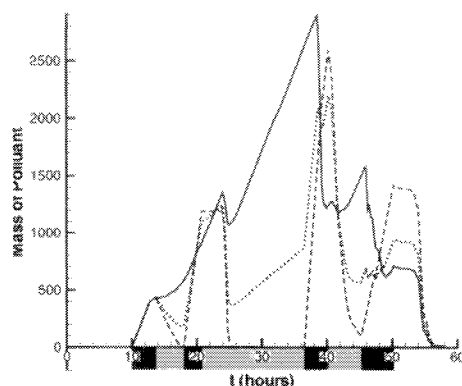


FIGURE 3. Total mass of contaminant in the coastal area for different source of pollution. The solid line is the result of pollution at a constant rate. The light and dark gray blocks on the x-axis are the zones identified by the DLE algorithm as respectively good release zones and bad release zones. The dashed line and dotted line are the result of optimized pollution release with respectively $\alpha = 0\%$ and $\alpha = 30\%$.

the half-period of the barrier point oscillation, during which contaminants should not be released. The contents of the tank are released once the barrier point passes south of the source of pollution. On Fig. 3 is the total mass of contaminant for the two release mode. Clearly, by getting information from the DLE plots, the white factory (dashed curve) is able to reduce by a factor of three the local contamination caused by the same amount of pollution.

Also shown on Fig. 3 is a 3rd experiment. In many case the damage to the environment is a function of the maximum concentration of contaminant. From this point of view our algorithm (releasing nothing during “dark gray” zones and as much as possible during “light gray” zone) does not seem to be efficient. The peak of maximum concentration for the white factory has only decreased by a small amount. To set up a more elaborate algorithm, we define a new degree of freedom α , the percentage of incoming created contaminant that will be released during “dark gray” zones. From this point of view, the black curve of Fig. 3 corresponds to $\alpha = 30\%$, the dashed curve to $\alpha = 0\%$ and the purple curve to $\alpha = 33\%$. Fig. 3 shows that a significant reduction of the peak of maximum concentration can be obtained using an appropriate partial release during zones that are marked dangerous by the DLE algorithm.

ACKNOWLEDGMENTS

The VHF radar data used in this paper was collected and analyzed at the Southern Florida Ocean Measurement Center (SFOMC) by Arthur Mariano and Edward Ryan. The authors are grateful to the Office of Naval Research and particularly to Manuel Fiadero for his support and advices. This research was funded by ONR grant N00014-97-1-0071.

CONCLUSION

We have shown the existence of a set of repelling material lines in radar data obtained from the Fort Lauderdale area on the Florida coast. We have also shown how these material lines can be used to minimize the effect of coastal pollution by determining optimal release times. This approach can be used for making predictions about the trajectories of buoyant contaminants or the trajectories of nearly Lagrangian tracers. The data source can be VHF radar data or any other current data source, such as data-assimilated ocean models that approximate the near-surface velocity field to some reasonable level of accuracy. The other advantage of using ocean models is that the velocity provided is 3D+1, thus we can explore the Lagrangian structures that develop at various depths. Since these types of models are becoming more readily available and configured for various areas, we are currently in the process of extending MANGEN to compute Lyapunov exponents for 3D+1 velocity data. A real-time experimental realization of our pollution release will be most important, and is planned for future work.

REFERENCES

1. Prah, F. G., Crecellus, E., and Carpenter, R., *Environ Sci Technol*, **18**, 687–693 (1984).
2. Rice, D. W., Seltnerich, C. P., Spies, R. B., and Keller, M. L., *Environmental Pollution*, **82**, 79–91 (1993).
3. Verschuere, K., *Handbook of Environmental Data on Organic Chemicals*, Van Nostrand Reinhold Co., New York, 1983.
4. Shay, L., Cook, T., Haus, B., Martinez, J., Peters, H., Mariano, A., VanLeer, J., Edgar, A., Smith, S., Soloviev, A., Weisberg, R., and Luther, M., *EOS, Transactions, American Geophysical Union*, **81** (19), 209–213 (2000).
5. Stirling, J. R., *Physica D*, **144**, 169–193 (2000).
6. Haller, G., *Physica D*, **149**, 248–277 (2001).
7. Coulliette, C., Lekien, F., Marsden, J., Haller, G., and Paduan, J., *Physical Review Letters* (2002).
8. Webb, T., and Tomlinson, R. B., *J. Env. Eng.*, **118**, 338–362 (1992).
9. Smith, R., *IMA J Appl Math*, **51**, 187–199 (1993).
10. Bikangaga, J. H., and Nussehi, V., *Water Res.*, **29**, 2367–2375 (1995).
11. Giles, R. T., *Water Res.*, **29**, 563–569 (1995).
12. Smith, R., *J. Hydraulic Eng.*, **124**, 117–122 (1998).
13. Prandle, D., *J. Phys. Oceanogr.*, **17**, 231–245 (1987).
14. Shay, H. C., L. K. and Graber, Ross, D. B., and Chapman, R. D., *J. Atmos. Ocean Tech.*, **12**, 881–900 (1995).
15. Stewart, R. H., and Joy, J. W., *Deep-Sea Res.*, **21**, 1039–1049 (1974).
16. Miller, P. D., Jones, C. K. R. T., Rogerson, A. M., and Pratt, L. J., *Physica D*, **110**, 1–18 (1997).
17. Poje, A. C., and Haller, G., *J. Phys. Oceanogr.*, **29**, 1649–1665 (1999).
18. Coulliette, C., and Wiggins, S., *Nonlinear Proc. Geophys.*, **8**, 69–94 (2001).
19. Ridderinkhof, H., and Zimmerman, J. T. F., *Science*, **258**, 1107–1111 (1992).
20. Lapeyre, G., Hua, B. L., and Legras, B., *Chaos*, **11**, 427– (2001).
21. Haller, G., *Phys. Fluids A*, **13**, 3368–3385 (2001).
22. Haller, G., *Phys. Fluids A*, **14**, 1851–1861 (2002).